Chemical Science

ROYAL SOCIETY OF CHEMISTRY

EDGE ARTICLE

View Article Online
View Journal | View Issue

Cite this: *Chem. Sci.*, 2025, **16**, 21852

All publication charges for this article have been paid for by the Royal Society of Chemistry

Heterologous expression of an *in planta*-upregulated gene cluster in the wheat pathogen *Parastagonospora nodorum* establishes the biosynthesis of methylene-bridged depsides

Hera T. Nguyen, [a] Nicolau Sbaraini, [a] Joe Bracegirdle, [a] Luke Smithers, [a] Stephen A. Moggach, [a] Daniel Vuong, [bc] Ernest Lacey, [bc] Peter S. Solomon, [d] Joel Haywood, [e] Andrew M. Piggott *[c] and Yit-Heng Chooi *[a]

Received 21st July 2025
Accepted 13th October 2025

DOI: 10.1039/d5sc05442g

rsc.li/chemical-science

Depsides are polyphenolic natural products commonly found in lichens, but also produced by some free-living fungi. Here, we report the discovery and functional characterisation of an *in planta*-upregulated biosynthetic gene cluster (*nds*) in the wheat fungal pathogen *Parastagonospora nodorum* SN15, comprising a non-reducing polyketide synthase (NR-PKS; NdsA), a non-ribosomal peptide synthetase (NRPS; NdsB) and a cytochrome P450 oxygenase (NdsC). Heterologous expression of the *nds* cluster in *Aspergillus nidulans* LO8030 yielded previously reported depsides, CJ-20,557 (**1**) and duricamidepside (**2**), alongside two novel dimeric methylene-bridged depsides, nodoraside A (**3**) and B (**4**). Combinatorial gene expression and precursor feeding experiments revealed that hydroxylation of CJ-20,557 by the cytochrome P450 NdsC, followed by non-enzymatic dehydration, generates an *ortho*-quinone methide intermediate, which reacts with a second depside unit to form methylene-bridged depsides. Notably, this crosslinking occurs only in the presence of NdsA and NdsB *in vivo*, indicating a possible requirement for protein–protein interactions or enzyme co-compartmentalisation. Methylene-bridged depside natural products are rare, and this study provides the first insight into their biosynthetic origin.

Introduction

Over the past 700 million years, fungi and plants have co-evolved, giving rise to complex interactions mediated by secondary metabolites. Depsides are a structurally diverse class of such metabolites, predominantly produced by lichens and some free-living fungi, and are known to exhibit phytotoxic and plant-modulating activities.[1,2] Structurally, depsides consist of two or more phenolic carboxylic acid units linked by ester bonds, and are typically assembled by type I iterative non-reducing polyketide synthases (NR-PKSs). A growing number of depsides produced by non-lichenised fungi have been identified, many of which display useful bioactivities.[3–10] Some of their biosynthetic pathways, particularly the formation of the depside linkage, have also begun to be deciphered.[3,6,11–13] In addition to variations in methylation patterns on the phenolic units introduced by NR-PKSs, further structural diversification of depsides often involves tailoring enzymes that mediate modifications such as amino acid incorporation (*e.g.*, amidation of amidepsine A with alanine), *O*-methylation (*e.g.*, *O*-methyl esterification of atranorin)[14] and glycosylation (*e.g.*, *O*-galactosylation of aquastatin A)[3] (Fig. 1). An uncommon structural feature observed in depsides is dimerisation *via* a methylene bridge. To date, the only known methylene-bridged dimeric depsides are thielocin B3 and its derivatives from *Thielavia terricola* RF-143, which were reported to be phospholipase A_2 inhibitors.[8] However, the molecular basis for their biosynthesis remain unresolved.

Methylene bridge formation in dimeric fungal natural products has been recently reviewed, highlighting that many such linkages form non-enzymatically through reactions involving an electrophilic C_1 unit, such as formaldehyde, produced endogenously by the host organisms.[15] For example, Shao *et al.* hypothesised that the methylene bridge in aspergilone B, produced by a marine-derived *Aspergillus* sp., arises *via* non-enzymatic nucleophilic addition of two molecules of debenzylaspergilone A to endogenous formaldehyde.[16] However, the mechanisms underlying the formation of such linkages in dimeric depsides remain unresolved.

[a]*School of Molecular Sciences, The University of Western Australia, Perth, WA 6009, Australia. E-mail: yitheng.chooi@uwa.edu.au*

[b]*Microbial Screening Technologies Pty. Ltd, Smithfield, NSW 2164, Australia*

[c]*School of Natural Sciences, Macquarie University, Sydney, NSW 2109, Australia. E-mail: andrew.piggott@mq.edu.au*

[d]*Research School of Biology, The Australian National University, Acton, ACT 2601, Australia*

[e]*Centre for Crop and Disease Management, School of Molecular and Life Sciences, Curtin University, WA 6102, Australia*

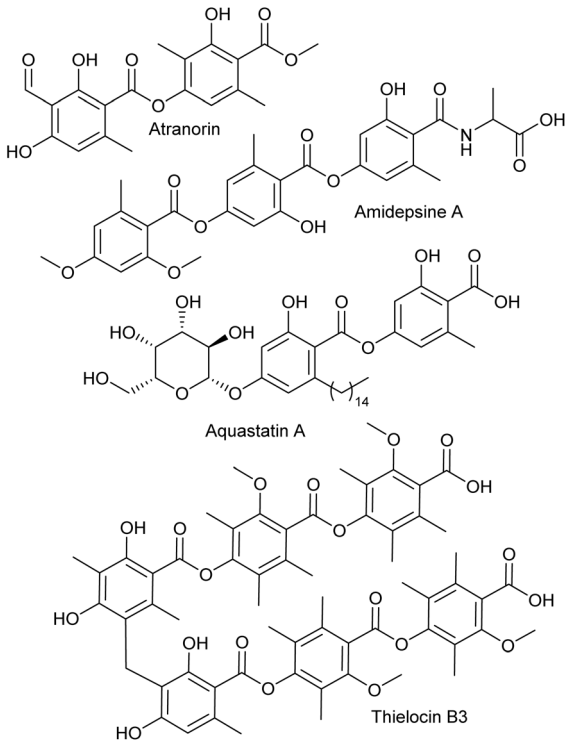

Fig. 1 Structures of depsides with diverse modifications, such as amidation, methylation and glycosylation.

Building on our ongoing research into fungal natural products associated with plant pathogens,[17–21] we have used a transcriptomics-guided strategy to identify bioactive metabolites involved in pathogen-plant interactions in the important wheat pathogen *Parastagonospora nodorum* SN15. Since many biosynthetic gene clusters (BGCs) encoding secondary metabolite production are conditionally expressed, an ecological genomics-guided approach leveraging transcriptomics data from pathogen–host interactions can help identify BGCs potentially involved in virulence or plant interactions.[22] Using this strategy, previous studies have uncovered phytotoxic metabolites from *P. nodorum* SN15, including perylenequinones (elsinochrome A and C),[19,23] dihydrofuran-linked α-pyrones,[20] and novel cytochalasans,[18] providing deeper insights into the ecological roles of fungal secondary metabolites in plant interactions.

In this study, we have reanalysed previously acquired transcriptomics data comparing *in planta* infection with axenic cultures of *P. nodorum* SN15,[22,24] leading to the identification of a candidate BGC (*nds*) that is potentially involved in host interactions. Through heterologous expression of the *nds* BGC, we discovered both previously reported depsides and novel methylene-bridged dimeric depsides. Based on additional insights gained from combinatorial gene expression, isolation of pathway intermediates, precursor feeding studies and NR-PKS domain mutagenesis experiments, we propose a new biosynthetic paradigm for methylene bridge formation between depside units.

Results and discussion

The *nds* cluster is conserved in other fungal plant pathogens

Ipcho *et al.*[24] have previously performed transcriptome analysis of *P. nodorum* SN15 during infection *in planta* on wheat (*Triticum aestivum*) and in axenic cultures (*in vitro*).[22,24] Analysis of the biosynthetic genes in the microarray transcriptomics dataset revealed an NR-PKS (SNOG_07020/JI435_070200) and a non-ribosomal peptide synthetase (NRPS) (SNOG_07021/JI435_070210) with increased expression levels *in planta*, peaking at 3 days post-inoculation (dpi) (Fig. S1). The peak expression level coincided with the development of plant tissue necrosis during *P. nodorum* infection.[22,24] Similarly, these two genes were also shown to be upregulated at 3 dpi *in planta* compared to *in vitro* expression in a separate RNAseq study.[25] The genomic co-localisation and co-regulation of both genes suggests that they participate in the same biosynthetic pathway.

To determine the boundaries of the *nds* BGC, we queried the NCBI GenBank database with protein sequences JI435_070170–JI435_070230 using cblaster.[26] This revealed that three genes—NR-PKS (JI435_070200; *ndsA*), NRPS (JI435_070210; *ndsB*) and cytochrome P450 (JI435_070190; *ndsC*)—have genomically co-localised homologues in multiple fungal plant pathogens, including *Alternaria alternata*, *Stemphylium lycopersici*, *Pyrenophora teres* f. *teres*, *Ascochyta lentis*, and *Clathrospora elynae* (Fig. S2). This suggests that *ndsA*, *ndsB* and *ndsC* constitute the core biosynthetic genes of the *nds* BGC in *P. nodorum*, and that metabolites encoded by this BGC may play a role in the plant pathogenic lifestyle of these fungi.

To determine the domain architecture of NdsA and NdsB, we queried their protein sequences using the NCBI conserved domain search (CDS).[27] The search revealed that the NdsA protein domain architecture consists of a starter-unit acyltransferase (SAT), ketosynthase (KS), acyltransferase (AT), product template (PT), two acyl carrier protein (ACP) domains, *C*-methyltransferase (cMT), and thioesterase (TE) domains (Fig. 2A), while the domain organisation of NdsB consists of adenylation (A), thiolation (T), and condensation (C) domains. Notably, the C domain of NdsB is followed by a ~100 amino acid region lacking any identifiable conserved domain (Fig. S3). Alphafold3 modelling[28] revealed that this region likely forms a long linker region and alpha-helical bundle that resembles a T domain, while FoldSeek[29] analysis confirmed it is structurally similar to known T domains (Fig. S3 and S4). The canonical GGXS motif, where the serine residue is normally post-translationally modified by a phosphopantetheinyl transferase (PPTase) to install a 4′-phosphopantetheine (PPant) arm crucial for substrate tethering,[30,31] is mutated to WGNG in NdsB, likely abolishing the catalytic function of the domain. Based on these observations, we designated this region as an inactive thiolation (T_i) domain and revised the domain organisation of NdsB to A, T, C, and T_i (Fig. 2A). Interestingly, the T_i domain is conserved in orthologous NRPSs of *S. lycopersici*, *P. teres* f. *teres*, *A. lentis*, and *C. elynae* (Fig. 2B). In these orthologues, the conserved glycine residue is also substituted with tryptophan, while the conserved serine residue is replaced by glycine or alanine

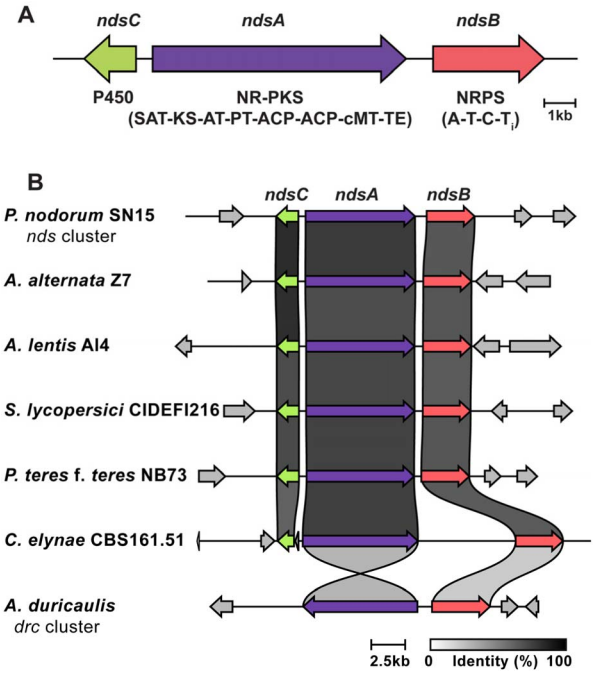

Fig. 2 (A) Schematic of the *nds* cluster and domain architectures of NdsA and NdsB. (B) Clinker[40] analysis showing conservation of the *nds* cluster in the fungal plant pathogens *Alternaria alternata*, *Ascochyta lentis*, *Stemphylium lycopersici*, *Pyrenophora teres* f. *teres* and *Clathrospora elynae*, and the low sequence identity of NdsA and NdsB to the *drc* cluster in *Aspergillus duricaulis*.

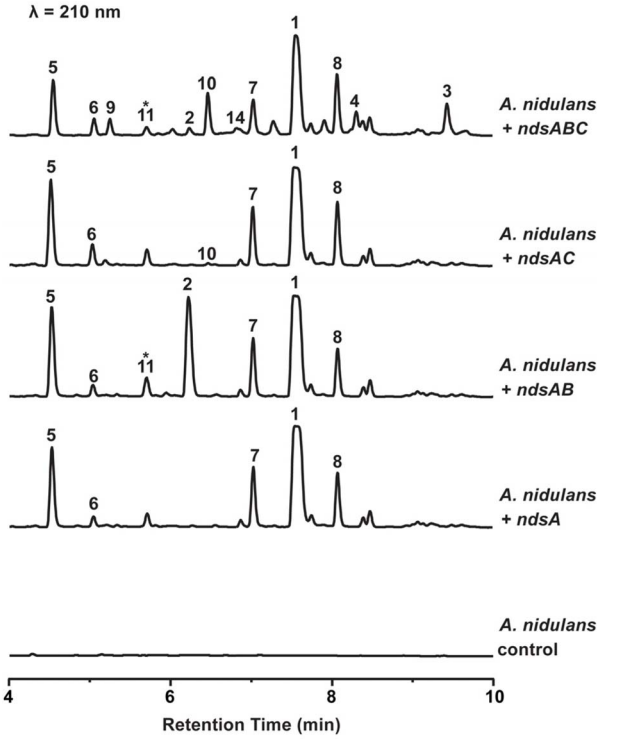

Fig. 3 Heterologous expression of the *nds* cluster in *Aspergillus nidulans* strain LO8030 produced compounds **1**–**11** and **14**. HPLC traces of extracts from *A. nidulans* transformants were monitored at 210 nm. *Peak consists of two compounds, one of which is **11**.

(Fig. S4). In contrast, the NRPS orthologue found in *A. alternata* retains the conserved serine but carries the glycine-to-tryptophan substitution (WGNS), which may still compromise the T domain activity (Fig. S4). The persistence of this T_i domain across species suggests a conserved, possibly structural or regulatory role, despite its loss of canonical catalytic function.

Co-expression of *ndsA* and *ndsB* in *Aspergillus nidulans* produces a suite of depsides

To investigate the metabolites produced by *nds* cluster, we performed heterologous reconstruction of the BGC in the engineered *Aspergillus nidulans* strain LO8030, which has low metabolic background.[32] The *ndsA*, *B* and *C* genes were cloned into pYFAC series AMA1-based expression plasmids, replacing the native promoters with *alc* promoters (P*alcA*, P*alcS*, and P*alcM*), which are inducible with alcohols or ketones and repressed by glucose.[19,33]

Heterologous expression of *ndsA* in *A. nidulans* produced compounds **1**, **5**–**8** based on LC-DAD-MS analysis (Fig. 3 and 4). HR-LC-ESI-MS (*m*/*z* 359.1130 $[M-H]^-$; $C_{19}H_{20}O_7$; Fig. S12 and S13) and NMR analyses of purified compound **1** revealed that its structure matched the previously described depside, CJ-20,557,[11,34] which consists of 3-methylorsellinic acid (3-MOA) and 3,5-dimethylorsellinic acid (DMOA) connected by a depside ester linkage (Fig. S17, S18 and Table S6). Compound **1** was first reported as a partial hydrolysis product of the tridepside, thielavin A,[34] and had been previously observed when *drcA*, an NR-PKS from the *Aspergillus duricaulis drc* gene cluster, was heterologously expressed in *Aspergillus oryzae* NSAR1.[11] Additionally, we isolated compounds **5** (*m*/*z* 181.0504 $[M-H]^-$; $C_9H_{10}O_4$; Fig. S12, S31, S32 and Table S10) and **6** (*m*/*z* 195.0660 $[M-H]^-$; $C_{10}H_{12}O_4$; Fig. S12, S33, S34 and Table S11) and elucidated their structures by NMR to be the monomeric units of **1**, *i.e.* 3-MOA and DMOA, respectively.

The structure of compound **7** (*m*/*z* 345.0974 $[M-H]^-$; $C_{18}H_{18}O_7$; Fig. S12 and S13) was elucidated by detailed spectroscopic analysis, revealing a novel depside consisting of orsellinic acid linked to DMOA *via* a depside ester bond (full structure elucidation in the SI; Fig. S35–S39 and Table S12). Compound **7** was named parastagonic acid. The structure of **8** (*m*/*z* 373.1289 $[M-H]^-$; $C_{20}H_{22}O_7$; Fig. S12 and S13) was elucidated by detailed spectroscopic analysis and single crystal X-ray diffraction (XRD) (Fig. S14, S40, S41 and Table S13), and was deduced to be identical to CJ-20,558, which has been previously generated through partial hydrolysis of thielavin A,[34] but has not been reported from a natural source. The isolation of three depsides with different methylation patterns (**1**, **7** and **8**) following expression of *ndsA* in *A. nidulans* demonstrates the ability of this NR-PKS to generate a range of products through depside coupling of different orsellinate monomers (orsellinic acid, **5** and **6**). This promiscuity was not observed by Chen *et al.* following expression of the NR-PKS *drcA* in *A. oryzae*.[11]

To investigate the function of the NRPS NdsB, *ndsB* was co-expressed with *ndsA* in *A. nidulans*, which in addition to

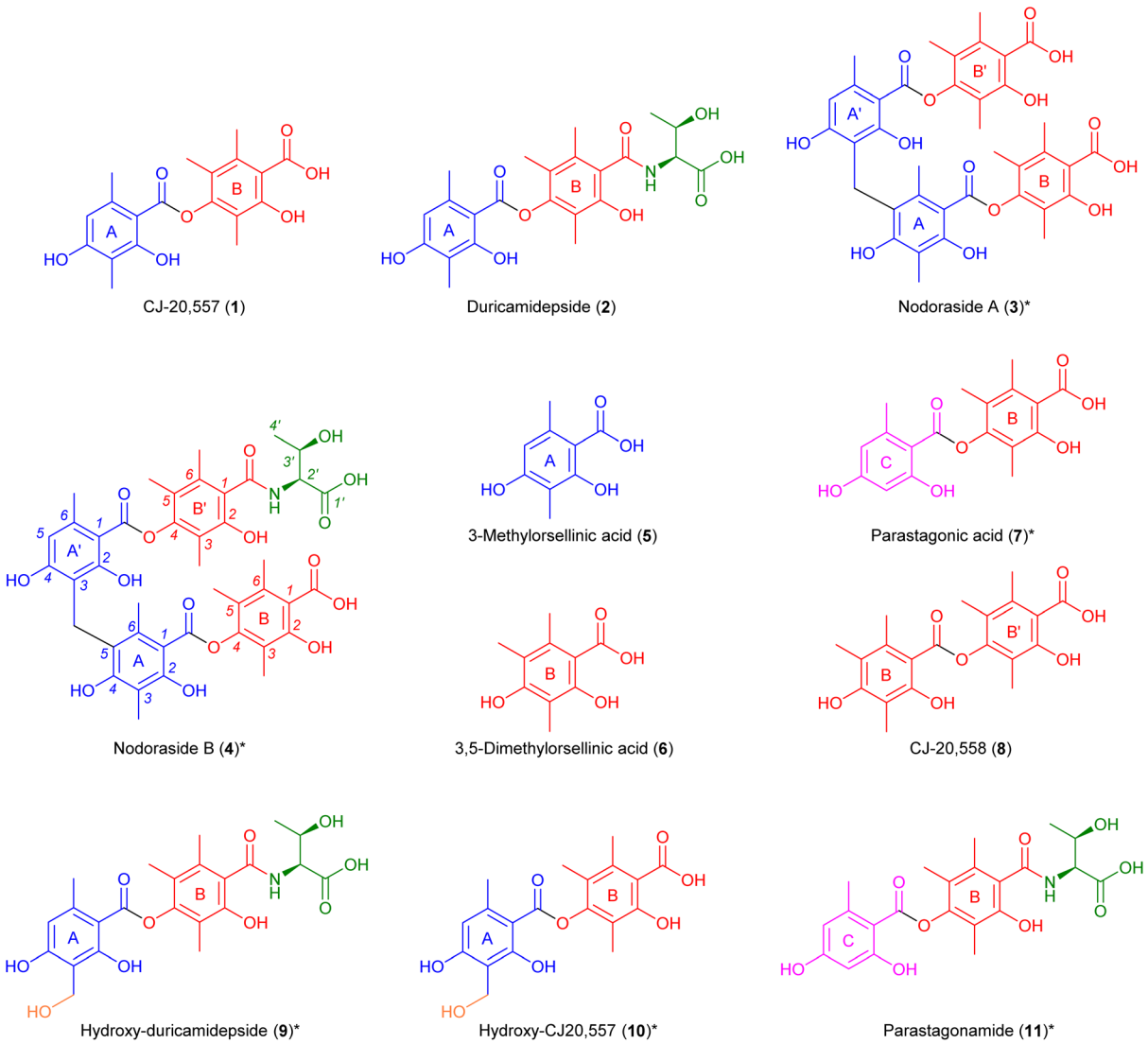

Fig. 4 Structures of **1–11** isolated from the heterologous expression of the *nds* cluster in *A. nidulans* LO8030. *Denotes novel compound identified in this study.

compounds **1**, **5–8**, yielded compounds **2** and **11** (Fig. 3 and 4). The structure of **2** (*m*/*z* 460.1610 $[M–H]^-$; $C_{23}H_{27}NO_9$; Fig. S12 and S13) was elucidated by detailed spectroscopic analysis to be the previously reported depside, duricamidepside,[11] which features L-threonine attached to the carbonyl group of the DMOA subunit of **1** *via* an amide bond (Fig. S19, S20 and Table S7). Compound **2** has also previously been obtained by co-expression of *A. duricaulis drcA* and NRPS, *drcB*, in *A. orzyae* NSAR1.[11] Furthermore, we isolated compound **11** (*m*/*z* 446.1453 $[M–H]^-$; $C_{22}H_{25}NO_9$; Fig. S12 and S13), which was elucidated by detailed spectroscopic analysis to be a novel depside consisting of orsellinic acid and DMOA, with L-threonine attached to the DMOA subunit (full structure elucidation in the SI; Fig. S52–S56 and Table S16). This is the first report of this amidated depside, which we named parastagonamide. Compound **11** co-eluted with another compound, which was observed in the *ndsA*-expressing strain (*m*/*z* 389.1238 $[M–H]^-$; $C_{20}H_{22}O_8$), but we were unable to isolate this compound in sufficient quantities for characterisation.

ndsC encoding a cytochrome P450 involved in hydroxylation and methylene bridge cross-linking of depsides

Comparison of the *nds* and *drc* clusters revealed that *ndsC* encodes a cytochrome P450 oxygenase not found in the *drc* cluster, suggesting that the *nds* cluster may produce depsides that undergo additional oxidative tailoring (Fig. 2B). Expression of *ndsABC* in *A. nidulans* produced four new compounds, **3**, **4**, **9** and **10** (Fig. 3 and 4) in addition to all those previously isolated.

HR-LC-ESI-MS (*m*/*z* 476.1562 $[M–H]^-$; $C_{23}H_{28}NO_{10}$; Fig. S12 and S13) and detailed spectroscopic analysis of compound **9** revealed the compound to be almost identical to **2**, except for hydroxylation of the 3-methyl group of the 3-MOA unit (full structure elucidation in the SI; Fig. S42–S46 and Table S14). Similarly, the structure of compound **10** (*m*/*z* 375.1084 $[M–H]^-$;

$C_{19}H_{20}O_8$; Fig. S12 and S13) was elucidated with detailed spectroscopic and XRD analysis, revealing a compound almost identical to **1**, except for hydroxylation of the 3-methyl group of the 3-MOA unit (full structure elucidation in the SI; Fig. S15, S47–S51 and Table S15). Thus, we have named **9** as hydroxy-duricamidepside and **10** as hydroxy-CJ20,557. The production of **9** and **10** by the *ndsABC*-expressing strain suggests that NdsC must be responsible for hydroxylation of the 3-methyl group of 3-MOA.

Intriguingly, we also isolated compounds **3** (*m*/*z* 717.2190 $[M–H]^-$; $C_{38}H_{38}O_{14}$; Fig. S12 and S13) and **4** (*m*/*z* 818.2663 $[M–H]^-$; $C_{42}H_{45}NO_{16}$; Fig. S12 and S13) from the *ndsABC*-expressing strain, which were both predicted to be dimerised depsides based on HR-LC-ESI-MS. Indeed, the NMR data for **3** revealed that it is a novel asymmetric dimer of **1**, crosslinked *via* a methylene bridge between C-5 of ring A and 3-Me of ring A′ (full structure elucidation in the SI; Fig. S21–S25 and Table S8). We named this new dimeric depside nodoraside A. Furthermore, the NMR data for compound **4** revealed that it was a novel asymmetric dimer of **1** and **2** crosslinked *via* a methylene group between C-5 of ring A and 3-Me of ring A′ (as seen in **3**) and with L-threonine attached to the carbonyl group of ring B′ (full structure elucidation in the SI; Fig. S26–S30 and Table S9). Subsequently, we named compound **4** as nodoraside B.

During our purification of **9** and **10**, we observed that these benzylic hydroxylated depsides were quite reactive, and in the presence of methanol, readily undergo methoxylation. When compound **9** was incubated overnight in methanol, a compound with a mass corresponding to a methyl ether analogue of **9** (compound **12**) was formed (Fig. 5 and S7), which we named methoxy-duricamidepside. Moreover, when purifying **10** with methanol, we isolated compound **13** (*m*/*z* 389.1235 $[M–H]^-$; $C_{20}H_{22}O_8$; Fig. S12 and S13), where its NMR and XRD data indicated it is a methyl ether **10**, which we named methoxy-CJ20,557 (Fig. 5; full structure elucidation in the SI; Fig. S16, S57–S61 and Table S17). Furthermore, we isolated another conversion product, compound **14** (*m*/*z* 640.2031 $[M–H]^-$; $C_{32}H_{34}NO_{13}$; Fig. S12 and S13), during our purification of **9**, where compounds **5** and **9** co-eluted. Drying these fractions from water containing 0.1% trifluoroacetic acid (TFA) and acetonitrile resulted in the formation of **14**. Detailed spectroscopic analysis of **14** revealed it to be compound **2** crosslinked to compound **5** *via* a methylene bridge between C-5 of ring A and 3-Me of ring A′ (as seen in **3** and **4**) (Fig. 5; full structure elucidation in the SI; Fig. S62–S66 and Table S18). Therefore, we named compound **14** as nodoraside C. Significantly, the production of **14** demonstrated that the methylene bridge crosslinking reaction can occur non-enzymatically *via* a benzylic hydroxylated intermediate produced by NdsC. On closer inspection, **14** could also be detected in low concentrations from *A. nidulans* expressing *ndsABC* but was absent in *A. nidulans* expressing *ndsA*, *ndsAC* and *ndsAB* (Fig. 3 and S68). This suggests that **14** can be biosynthesised *in vivo* but only in the presence of NdsA, NdsB and NdsC.

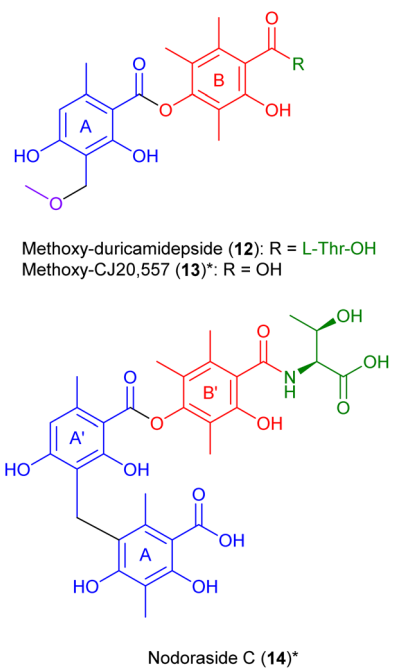

Fig. 5 Structures of conversion products **12**–**14** formed during the purification of hydroxy-duricamidepside (**9**) and hydroxy-CJ20,557 (**10**). *Denotes novel compound identified in this study.

Interestingly, expression of *ndsAC* (without *ndsB*) in *A. nidulans* did not produce the depside dimer **3**, with only trace amounts of benzyl alcohol **10** being detected. Notably, when *ndsB* was co-expressed (*ndsABC*), the production of **10** increased 13-fold (Fig. S8) and **9** was detected along with the methylene-bridged depsides **3** and **4** (Fig. 3). This suggests that the hydroxylation activity of NdsC and the production of methylene-bridged depsides are partially dependent on the presence of the NRPS NdsB.

Given the reactivities of **9** and **10**, as supported by the detection of the methoxylated compound **12** and isolation of the methoxylated compound **13** and 3-MOA-linked compound **14**, we hypothesise that these hydroxylated depsides are precursors for the formation of the methylene-bridged depsides **3** and **4**. To further investigate the potential dependency of the NdsC-catalysed hydroxylation and methylene bridge formation on the presence of NdsB, we fed **1** to *A. nidulans* strains expressing *ndsB* only and *ndsBC*, and fed either **1** or **2** to *ndsC*-expressing *A. nidulans* (Fig. S9). Feeding **1** to the *ndsB*-expressing transformant resulted in the production of L-threonine-amidated compound **2**, confirming that **1** can cross the cell membrane of *A. nidulans* and be used as a substrate by NdsB. However, feeding either **1** or **2** to *ndsC*-expressing strains did not yield hydroxylated compounds **9** and **10**, nor did it yield methylene-bridged compounds **3** and **4**. Production of hydroxylated compounds **9** and **10** was observed only when feeding **1** to *ndsBC*-expressing strains, which strengthens our hypothesis that NdsB is important for the function of NdsC. Unexpectedly, the methylene-bridged compounds **3** and **4** were not observed when **1** was fed to *ndsBC*-expressing strain, suggesting that NdsA may also be required for the dimerisation of the depsides.

To complement the feeding experiments on *ndsBC*-expressing strains, we attempted to reconstitute the enzymatic steps of

hydroxylation and methylene bridge formation *in vitro* using cell-free lysate of *A. nidulans* expressing *ndsB* and *ndsC* (Fig. S69). Consistent with the feeding assays, incubating **1** in lysate containing NdsB, as well as in an equal mixture of lysates containing NdsB and NdsC, resulted in the production of **2**. Similarly to the feeding assays, when **1** or both **1** and **2** were incubated in lysate containing NdsC alone, neither the hydroxylated compounds (**9** and **10**), nor the methylene-bridged compounds (**3** or **4**), were detected. Surprisingly, neither the methylene-bridged compounds **3** or **4**, nor the hydroxylated compounds **9** and **10**, were detected when **1** was incubated in a mixture of lysates containing NdsB and NdsC. It is possible this may be due to NdsC being inactivated in the process of preparing of the cell-free lysate.

As the feeding assays suggest cooperation of NdsB and NdsC for hydroxylation, we hypothesise that the catalytically inactive T_i domain in NdsB may be involved in the interaction with NdsC. To assess the role of the T_i domain, we deleted the T_i domain of *ndsB*, including the preceding linker region, and co-expressed the mutant with *ndsA* and *ndsC* in *A. nidulans*. Surprisingly, removal of the T_i domain abolished the production of **2**, **9** and **11** containing an L-threonine moiety and methylene-bridged depsides **3** and **4**, with only **1**, **5–8**, and trace amount of **10** produced, similar to *A. nidulans* expressing *ndsAC* only (Fig. S6). This suggests that the T_i domain is important for the amidation activity of NdsB and effective hydroxylation of **1** by NdsC.

Additionally, feeding assays with *A. nidulans* expressing *ndsBC* also suggest that NdsA is important for methylene bridge formation. We hypothesise that NdsA facilitates this step by bringing **1** into proximity with hydroxylated-**1** (**10**) tethered on NdsB, perhaps *via* its ACP domains. To investigate this, we inactivated the ACP domains by mutating the conserved serine residues, where the PPTase installs the PPant arm, to alanine (ACP-1 S1673A and/or ACP-2 S1796A), thereby abolishing substrate tethering (Fig. S70 and S71). As expected, mutating both ACP domains resulted in a non-functional NdsA and no compounds from the *nds* cluster were detected. Intriguingly, comparison of the ACP-1 mutant to the wildtype showed that the production of **1** decreased by 15.8-fold, while the hydroxylated compounds **9** and **10** decreased by 3.2-fold and 9.9-fold, respectively. Moreover, methylene-bridged compounds **3**, **4**, and **14** were not detected. However, in the ACP-2 mutant expression, the overall production of the *nds* compounds was reduced relative to the wildtype, but the methylene-bridged compounds **3** and **4**, and trace amounts of **14** were still detected. These results further corroborate our hypothesis that NdsA, specifically the ACP-1 domain, is involved in methylene bridge formation, potentially through protein–protein interaction or co-compartmentalisation with NdsB.

As the methylene bridge in **14** was formed non-enzymatically during the purification of **9**, we sought to replicate these conditions to investigate the formation of the methylene-bridged depside **4**. To this end, we reacted **1** and **9** in 50% aqueous acetonitrile, with and without 0.1% TFA, for 16 h at room temperature and then dried the reaction mixtures *in vacuo*. Compound **4** was detected under both conditions, although its yield was 6.5-fold higher in the presence of TFA (Fig. S10), suggesting that acidic conditions facilitate the dimerisation reaction, which may be facilitated *in vivo* by an acidic residue within the enzyme active site.

Proposed biosynthetic pathway for methylene bridge formation involves potential protein–protein interactions

In most of the fungal methylene-bridged dimeric natural products with elucidated biosynthetic pathways, the methylene bridge is formed non-enzymatically using a one-carbon donor, such as formaldehyde.[15,16,35–38] In contrast, we describe here an enzymatically initiated pathway for methylene bridge formation between two depside units, highlighting a novel biosynthetic strategy. We propose that methylene bridge formation is initiated by the cytochrome P450 oxygenase NdsC, which hydroxylates the 3-methyl group of the 3-MOA unit in depsides (**1** or **2**), yielding a benzyl alcohol. This intermediate undergoes non-enzymatic dehydration to form a reactive *ortho*-quinone methide (*o*-QM) intermediate, which then reacts with the aromatic methine *ortho* to the phenol on another depside **1** molecule, resulting in the formation of the methylene bridge observed in **3** and **4** (Fig. 6).

Methylene bridge formation *via* an *o*-QM intermediate has been previously reported in the non-dimeric natural products penilactone and peniphenone from *Penicillium crustosum* PRB-2.[39] Within this pathway, the *o*-QM is derived from hydroxyclavatol, which is generated by hydroxylation of clavatol (2′,4′-dihydroxy-3′,5′-dimethyl-acetophenone). Similar to compounds **9** and **10**, hydroxyclavatol contains a reactive benzyl alcohol, which can dehydrate to form a corresponding *o*-QM intermediate that reacts with tetronic acid intermediates to form the final methylene-bridged products.[39] Notably, in contrast to the nodoraside pathway described here, this benzylic hydroxylation is catalysed by a non-heme iron (Fe^{II})/2-oxoglutarate-dependent oxygenase rather than a cytochrome P450 oxygenase.

As proposed previously by Chen *et al.* for DrcB,[11] our findings suggest that NdsB activates **1** and incorporates L-threonine to generate the amide **2**. However, formation of **3** and **4**—unique to the *nds* cluster—was observed only when co-expressing *ndsA*, *ndsB* and *ndsC*, indicating that all three enzymes are required for methylene bridge formation. Based on these results, we propose that the cytochrome P450 oxygenase NdsC hydroxylates the thioester form of **1** while it is tethered to the T domain of NdsB, forming NdsB-**10** (Fig. 6). The benzyl alcohol of NdsB-**10** then undergoes non-enzymatic dehydration to yield a reactive *o*-QM, which subsequently reacts with a second molecule of depside **1**-thioester tethered to ACP-1 of NdsA *via* conjugate addition. Formation of the methylene bridge while **10** is tethered on the NRPS is supported by the absence of an isomer of **4** with L-threonine attached to the carbonyl group of ring B rather than ring B′. The role of NdsA in facilitating the dimerisation is also supported by the absence of methylene-bridged depsides **3** and **4** when **1** is fed to *A. nidulans* expressing *ndsBC* (without *ndsA*), even though the hydroxylated intermediates **9** and **10** were detected. Furthermore, production of **3** and **4** was abolished in our heterologous expression of *ndsBC* with the *ndsA*

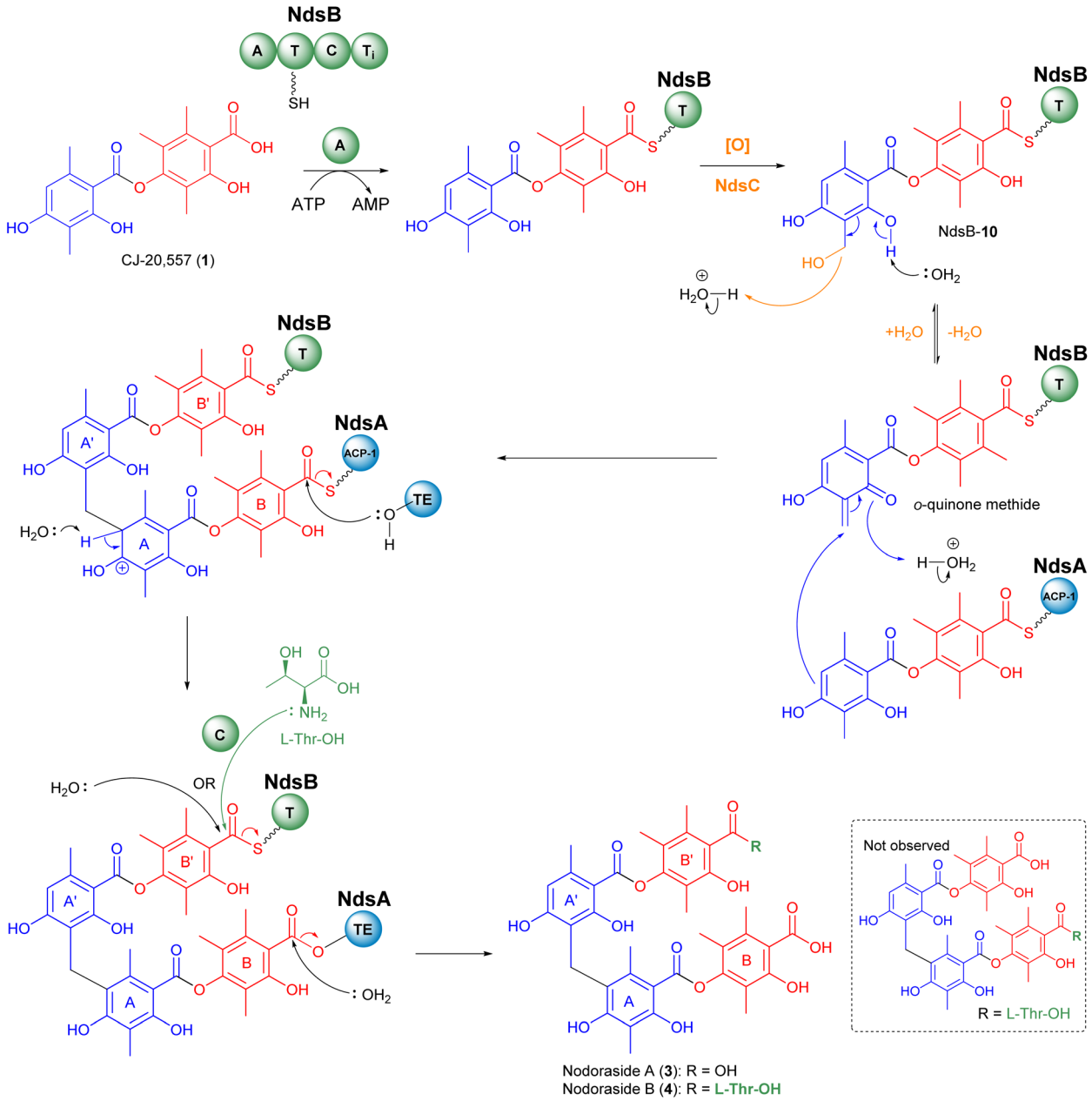

Fig. 6 Proposed biosynthetic pathway to nodoraside A (**3**) and nodoraside B (**4**).

ACP-1 (S1673A) mutant. Following the *o*-QM-mediated C–C bond formation, rearomatisation of ring A and hydrolysis of the thioester by the TE domain releases the cross-linked product from NdsA. The final step is determined by NdsB, which either hydrolyses the product from the T domain to generate **3**, or condenses it with L-threonine to yield **4**, catalysed by the C domain (Fig. 6).

Interestingly, although DrcA and DrcB from *A. duricalis* produce the same compounds **1** and **2**, they share low protein sequence identity with NdsA (39%) and NdsB (32%), respectively (Fig. S5). This is in contrast with the other homologous BGCs in dothideomycete plant pathogens identified by cblaster, where the overall protein sequence identities with NdsA and NdsB were >70% (Table S1). On close inspection, the T_i domain found in NdsB was also conserved in DrcB, except for the serine residue, which has been replaced with leucine (WGDL) (Fig. S4). We investigated whether the cytochrome P450 oxygenase NdsC could functionally interact with the *A. duricaulis* enzymes DrcA and DrcB in the *A. nidulans* host. Surprisingly, despite both the low sequence homology between DrcAB and NdsAB, and the absence of a *ndsC* orthologue in the *drc* cluster, production of both **3** and **4** was observed in *A. nidulans* expressing *drcA*, *drcB* and *ndsC* (Fig. S11). This suggests that NdsC may exhibit promiscuity in its interactions with PKSs or NRPSs, potentially *via* recognition of conserved features in carrier protein domains. Supporting NdsC promiscuity to interact with carrier

proteins other than the NRPS, trace amounts of benzyl alcohol-containing compound **10** were detected when *ndsAC* were co-expressed, suggesting that NdsC may also hydroxylate **1**-thioester tethered to the ACP domains of NdsA to a small extent. Alternatively, formation of the dimer may result from co-compartmentalisation of DrcA and DrcB with NdsC in *A. nidulans*, enabling proximity-based catalysis.

Bioactivity of the isolated compounds

Lastly, we investigated whether the isolated compounds derived from the *nds* BGC exhibit herbicidal activity. Initially, we performed a pre-emergence treatment on the model dicot, *Arabidopsis thaliana*, grown on 0.1% agar with varying concentrations of **1–4**, **7–8**, with glyphosate as a positive control. Compounds **1** and **7** showed weak herbicidal activities against *A. thaliana* at 200 μM and 400 μM, respectively (Fig. S67). We also assessed herbicidal activity of **1–4** against the model monocot, *Eragrostis tef*, with abscisic acid as the control. However, none of the compounds displayed activity against *E. tef* (Table S2). Additionally, we performed detached leaf assays (DLA) of *P. nodorum* infecting wheat leaves to determine if these metabolites are produced during infection. However, at 5 dpi, we were unable to detect these metabolites in our chemical extraction of the infected leaves (results not shown). However, these compounds could still have a role in modulating plant pathway, but further experiments would be required to assess this. Finally, we assessed the minimum inhibitory concentrations (MICs) of **1–4** against *Bacillus subtilis* and *Staphylococcus aureus* (antibacterial activity), *Candida albicans* and *Saccharomyces cerevisiae* (antifungal activity), and cytotoxicity against mouse myeloma NS-1 cells. Compound **1** displayed antibacterial activity against *B. subtilis* (25 μg mL^{-1}) and antifungal activity against *C. albicans* (25 μg mL^{-1}), with no cytotoxicity (Table S2). These results suggest that compound **1** may act on multiple molecular targets that differ between bacterium and eukaryote.

Conclusions

To our knowledge, this is the first report describing the biosynthetic mechanism for methylene bridge formation between two depsides. Using a transcriptomics-guided genome mining approach, heterologous expression and feeding assays, we characterised the *nds* BGC from *P. nodorum* and isolated depside metabolites for the first time from this important wheat pathogen. In this study, we isolated eight novel depsides (compounds **3**, **4**, **7**, **9**, **10**, **11**, **13**, **14**), one depside for the first time as a natural product (compound **8**), and two previously reported depsides (compounds **1** and **2**). Significantly, we have shed light on the biosynthetic mechanism involved in the formation of methylene-bridged depsides, where the mechanism is initiated by hydroxylation of **1** by NdsC. Although methylene-bridged depsides such as thielocin B3 have been previously isolated from fungi, this study has provided the first direct evidence linking a specific enzyme to methylene bridge formation. While further studies are needed to determine whether orthologues of NdsC could catalyse dimerisation in other methylene-bridged depsides, our results point towards a conserved mechanistic paradigm. The knowledge gained here reveals an alternative biosynthetic strategy for constructing methylene-bridged dimeric fungal natural products, distinct from previously described non-enzymatic mechanisms involving host-derived formaldehyde[15] and expands biosynthetic strategies for diversification of natural product scaffolds. Notably, Nature has evolved distinct enzymatic strategies to exploit *o*-QM intermediates in C–C bond formation, as seen in penilactone and peniphenone biosynthesis *via* a non-heme Fe^{II}/2-oxoglutarate-dependent oxygenase and in the P450-mediated pathway described here. Furthermore, we identified the T_i domain in NdsB and suggested it may have a role for the function of NdsB and in potentially mediating its interaction with NdsC. Biochemical validation for the role of the T_i domain is currently in progress. Additionally, evidence from combinatorial gene expression, ACP domain mutagenesis, and feeding assays suggests that the methylene bridge formation requires either protein–protein interaction of all three proteins or enzyme co-compartmentalisation. Further work is also underway to investigate this hypothesis.

Finally, although we could not detect the metabolites produced by the *nds* cluster *in planta*, the weak herbicidal activity observed for some depsides suggested potential ecological relevance in plant–pathogen interactions. Further studies assessing their biological role in *P. nodorum* could provide important insights into fungal–host dynamics and the functional significance of such depsides in fungal biology. Additionally, our findings will facilitate the discovery of related methylene-bridged depsides in other fungi, deepening our understanding of their biosynthetic diversity and evolutionary origins.

Author contributions

Conceptualisation – HTN, NS, and YHC; investigation – HTN, NS, JB, LS, SAM, DV, EL, PSS, JH, and AMP; data curation – HTN, NS, JB, LS, SAM, DV, JH, and AMP; formal analysis – HTN, JB, LS, SAM, JH, AMP and YHC; funding acquisition – SAM, EL, AMP, and YHC; supervision – NS, AMP, and YHC; writing – original draft – HTN, NS, JB, LS, JH and YHC; writing – review & editing – JB, AMP, and YHC.

Conflicts of interest

The authors declare that the research was conducted in the absence of any commercial or financial relationships that could be construed as a potential conflict of interest.

Data availability

CCDC 2444315, 2473101 and 2473102 contain the supplementary crystallographic data for this paper.[41a–c]

All experimental procedures, and additional experimental and characterisation data are available in the supplementary information (SI). Supplementary information: experimental procedures and additional data for structure elucidations,

heterologous expression, precursor feeding experiments, bioactivity screening, conservation analysis, protein modelling and spectroscopic analysis. See DOI: https://doi.org/10.1039/d5sc05442g.

Acknowledgements

This study was funded by the Australian Research Council (ARC) (LP210100458) and the Grains Research and Development Corporation (GRDC) *via* a GRDC Scholarship (UWA2306-003RSX). Y.-H. C. is supported by an ARC Mid-Career Industry Fellowship (IM230100154). H. T. N. is supported by an Australian Research Training Program (RTP) Scholarship and GRDC Scholarship. We would like to thank Prof. Berl R. Oakley (University of Kansas) for gifting the *A. nidulans* strain LO8030 and Prof. Max J. Cryle, A./Prof. Robert Tuckey and Dr Jinyu Hu for helpful discussions. HR-MS and NMR were performed at the UWA Separation Science & Mass Spectrometry Platform (LE210100110) and the UWA Centre for Microscopy Characterisation & Analysis (CMCA) (ARC LE190100183). X-ray diffraction was performed at the UWA X-ray Diffraction Facility (LE170100199). The preparative LC used in this study was supported by the Western Australia Future Health Research & Innovation Infrastructure Fund (FHRIFGCOVID19/14).

Notes and references

1 M. Bačkor, M. Goga, D. Ručová, D. Urminská, M. Bačkorová and B. Klejdus, *S. Afr. J. Bot.*, 2023, **162**, 688–693.
2 T. Endo, T. Takahagi, Y. Kinoshita, Y. Yamamoto and F. Sato, *Biosci. Biotechnol. Biochem.*, 1998, **62**, 2023–2027.
3 N. Sbaraini, A. Crombie, J. A. Kalaitzis, D. Vuong, J. Bracegirdle, F. Windsor, A. Lau, R. Chen, Y. P. Tan, A. Lacey, E. Lacey, A. M. Piggott and Y.-H. Chooi, *Chem. Sci.*, 2024, **15**, 18872–18880.
4 A. Crombie, J. A. Kalaitzis, R. Chen, D. Vuong, A. E. Lacey, E. Lacey, R. G. Shivas, Y. P. Tan, N. Sbaraini, Y.-H. Chooi and A. M. Piggott, *J. Antibiot.*, 2024, **77**, 639–646.
5 N. Kitahara, A. Endo, K. Furuya and S. Takahasi, *J. Antibiot.*, 1981, **34**, 1562–1568.
6 Q. Liu, D. Zhang, S. Gao, X. Cai, M. Yao, Y. Xu, Y. Gong, K. Zheng, Y. Mao, L. Yang, D. Yang, I. Molnár and X. Yang, *Angew. Chem., Int. Ed.*, 2023, **62**, e202214379.
7 Y. Chen, W. Yang, G. Zou, S. Chen, J. Pang and Z. She, *Fitoterapia*, 2019, **139**, 104369.
8 K. Tanaka, S. Matsutani, A. Kanda, T. Kato and T. Yoshida, *J. Antibiot.*, 1994, **47**, 631–638.
9 C. W. Johnson, L. Nuniz, B. Perlatti, G. F. Bills and Y. Tang, *ChemBioChem*, 2025, **26**, e202500003.
10 X. Zhang, L. Liu, J. Huang, X. Ren, G. Zhang, Q. Che, D. Li and T. Zhu, *Mar. Drugs*, 2025, **23**, 130.
11 L. Chen, X. Wei and Y. Matsuda, *J. Am. Chem. Soc.*, 2022, **144**, 19225–19230.
12 Q. Ji, H. Xiang, W. Wang and Y. Matsuda, *Angew. Chem., Int. Ed.*, 2024, **136**, e202402663.
13 H. Yang, Z. Shang, Y. Chen, F. Li, K. Li, H. Zhu, M. Peng, J. Yang, C. Cai and J. Ju, *Org. Lett.*, 2024, **26**, 8317–8322.
14 W. Kim, R. Liu, S. Woo, K. Bin Kang, H. Park, Y. H. Yu, H.-H. Ha, S.-Y. Oh, J. H. Yang, H. Kim, S.-H. Yun and J.-S. Hur, *mBio*, 2021, **12**, e0111121.
15 Y. Fan, J. Shen, Z. Liu, K. Xia, W. Zhu and P. Fu, *Nat. Prod. Rep.*, 2022, **39**, 1305–1324.
16 C.-L. Shao, C.-Y. Wang, M.-Y. Wei, Y.-C. Gu, Z.-G. She, P.-Y. Qian and Y.-C. Lin, *Bioorg. Med. Chem. Lett.*, 2011, **21**, 690–693.
17 S. C. Kessler, X. Zhang, M. C. McDonald, C. L. M. Gilchrist, Z. Lin, A. Rightmyer, P. S. Solomon, B. G. Turgeon and Y.-H. Chooi, *Proc. Natl. Acad. Sci. U. S. A.*, 2020, **117**, 24243–24250.
18 H. Li, H. Wei, J. Hu, E. Lacey, A. N. Sobolev, K. A. Stubbs, P. S. Solomon and Y.-H. Chooi, *ACS Chem. Biol.*, 2020, **15**, 226–233.
19 J. Hu, F. Sarrami, H. Li, G. Zhang, K. A. Stubbs, E. Lacey, S. G. Stewart, A. Karton, A. M. Piggott and Y.-H. Chooi, *Chem. Sci.*, 2019, **10**, 1457–1465.
20 H. Li, J. Hu, H. Wei, P. S. Solomon, D. Vuong, E. Lacey, K. A. Stubbs, A. M. Piggott and Y.-H. Chooi, *Org. Lett.*, 2018, **20**, 6148–6152.
21 R. Darma, Z. Shang, J. Bracegirdle, S. Moggach, M. C. McDonald, A. M. Piggott, P. S. Solomon and Y.-H. Chooi, *ACS Chem. Biol.*, 2025, **20**, 421–431.
22 Y.-H. Chooi and P. S. Solomon, *Front. Microbiol.*, 2014, **5**, 640.
23 Y. Chooi, G. Zhang, J. Hu, M. J. Muria-Gonzalez, P. N. Tran, A. Pettitt, A. G. Maier, R. A. Barrow and P. S. Solomon, *Environ. Microbiol.*, 2017, **19**, 1975–1986.
24 S. V. S. Ipcho, J. K. Hane, E. A. Antoni, D. Ahren, B. Henirissat, T. L. Friesen, P. S. Solomon and R. P. Oliver, *Mol. Plant Pathol.*, 2012, **13**, 531–545.
25 D. A. B. Jones, E. John, K. Rybak, H. T. T. Phan, K. B. Singh, S.-Y. Lin, P. S. Solomon, R. P. Oliver and K.-C. Tan, *Sci. Rep.*, 2019, **9**, 15884.
26 C. L. M. Gilchrist, T. J. Booth, B. van Wersch, L. van Grieken, M. H. Medema and Y.-H. Chooi, *Bioinform. Adv.*, 2021, **1**, vbab016.
27 J. Wang, F. Chitsaz, M. K. Derbyshire, N. R. Gonzales, M. Gwadz, S. Lu, G. H. Marchler, J. S. Song, N. Thanki, R. A. Yamashita, M. Yang, D. Zhang, C. Zheng, C. J. Lanczycki and A. Marchler-Bauer, *Nucleic Acids Res.*, 2023, **51**, D384–D388.
28 J. Abramson, J. Adler, J. Dunger, R. Evans, T. Green, A. Pritzel, O. Ronneberger, L. Willmore, A. J. Ballard, J. Bambrick, S. W. Bodenstein, D. A. Evans, C.-C. Hung, M. O'Neill, D. Reiman, K. Tunyasuvunakool, Z. Wu, A. Žemgulytė, E. Arvaniti, C. Beattie, O. Bertolli, A. Bridgland, A. Cherepanov, M. Congreve, A. I. Cowen-Rivers, A. Cowie, M. Figurnov, F. B. Fuchs, H. Gladman, R. Jain, Y. A. Khan, C. M. R. Low, K. Perlin, A. Potapenko, P. Savy, S. Singh, A. Stecula, A. Thillaisundaram, C. Tong, S. Yakneen, E. D. Zhong, M. Zielinski, A. Žídek, V. Bapst, P. Kohli, M. Jaderberg, D. Hassabis and J. M. Jumper, *Nature*, 2024, **630**, 493–500.

29 M. van Kempen, S. S. Kim, C. Tumescheit, M. Mirdita, J. Lee, C. L. M. Gilchrist, J. Söding and M. Steinegger, *Nat. Biotechnol.*, 2024, **42**, 243–246.
30 K. Bloudoff and T. M. Schmeing, *Biochim. Biophys. Acta, Proteins Proteomics*, 2017, **1865**, 1587–1604.
31 R. H. Lambalot, A. M. Gehring, R. S. Flugel, P. Zuber, M. LaCelle, M. A. Marahiel, R. Reid, C. Khosla and C. T. Walsh, *Chem. Biol.*, 1996, **3**, 923–936.
32 Y. Chiang, M. Ahuja, C. E. Oakley, R. Entwistle, A. Asokan, C. Zutz, C. C. C. Wang and B. R. Oakley, *Angew. Chem., Int. Ed.*, 2016, **55**, 1662–1665.
33 I. Roux and Y. H. Chooi, in *Engineering Natural Product Biosynthesis: Methods and Protocols*, ed. E. Skellam, Humana, New York, NY, 2022, pp. 75–92.
34 S. Sakemi, H. Hirai, T. Ichiba, T. Inagaki, Y. Kato, N. Kojima, H. Nishida, J. C. Parker, T. Saito, H. Tonai-Kachi, M. A. Vanvolkenburg, N. Yoshikawa and Y. Kojima, *J. Antibiot.*, 2002, **55**, 941–951.
35 X. Y. Wu, X. H. Liu, Y. C. Lin, J. H. Luo, Z. G. She, L. Houjin, W. L. Chan, S. Antus, T. Kurtan, B. Elsässer and K. Krohn, *Eur. J. Org Chem.*, 2005, **2005**, 4061–4064.
36 D. Bellis, M. Spring and J. Stoker, *Biochem. J.*, 1967, **103**, 202–206.
37 L. Du, D. Li, G. Zhang, T. Zhu, J. Ai and Q. Gu, *Tetrahedron*, 2010, **66**, 9286–9290.
38 W. J. Andrioli, R. Conti, M. J. Araújo, R. Zanasi, B. C. Cavalcanti, V. Manfrim, J. S. Toledo, D. Tedesco, M. O. de Moraes, C. Pessoa, A. K. Cruz, C. Bertucci, J. Sabino, D. N. P. Nanayakkara, M. T. Pupo and J. K. Bastos, *J. Nat. Prod.*, 2014, **77**, 70–78.
39 J. Fan, G. Liao, F. Kindinger, L. Ludwig-Radtke, W.-B. Yin and S.-M. Li, *J. Am. Chem. Soc.*, 2019, **141**, 4225–4229.
40 C. L. M. Gilchrist and Y.-H. Chooi, *Bioinformatics*, 2021, **37**, 2473–2475.
41 (*a*) CCDC 2444315: Experimental Crystal Structure Determination, 2025, DOI: **10.5517/ccdc.csd.cc2n1hw3**; (*b*) CCDC 2473101: Experimental Crystal Structure Determination, 2025, DOI: **10.5517/ccdc.csd.cc2p0ggn**; (*c*) CCDC 2473102: Experimental Crystal Structure Determination, 2025, DOI: **10.5517/ccdc.csd.cc2p0ghp**.